# Phenomenological approach towards modelling the acoustic emission due to plastic deformation in metals

A. Vinogradov[1*], I.S. Yasnikov[2] and D.L. Merson[2]

[1] Department of Mechanical and Industrial Engineering, Norwegian University of Science and Technology - NTNU, 7491 Trondheim, Norway

[2]Institute of Advanced Technologies, Togliatti State University, Togliatti, 445020 Russia

*Corresponding author: alexei.vinogradov@ntnu.no

**Abstract.** Considering acoustic emission (AE) as a phenomenon reflecting the elastic energy dissipation process in deforming metals, a simple yet self-consistent model is proposed to account for the AE behaviour accompanying microstructure evolution during uniform plastic deformation of metals. The relationship between the AE power, mobile dislocation density and plastic flow characteristic parameters - the strain hardening rate and flow stress - is derived and experimentally verified for face centred cubic metals with different stacking fault energies (SFE). Despite its simplicity, the proposed purely phenomenological relation captures most of the salient features of the AE behaviour of early deformation stages in metals.

**Keywords:** acoustic emission; dislocation slip; microstructure evolution; phenomenological model

Plastic flow in a deforming crystal is a dissipative process driven by external stress as a function of time. Among the modern in-situ techniques, which can resolve the dynamics of physical processes underlying plastic deformation, acoustic emission (AE) has been widely recognized for its unprecedented sensitivity to elementary mechanisms of plasticity. Being of the order of a microsecond, the temporal resolution of the AE method is superior to many other known in-situ techniques. AE detects transient elastic waves generated by rapid energy release from localised sources within the material. Various dislocation reactions including breaking away from pinning points, co-operative motion, annihilation and escaping to a free surface are among the detectable AE sources. Therefore, the potential of AE measurements as a deformation characterisation tool enjoys growing recognition nowadays [1-4].

There is a long history of works, getting back to 1960s, that documented the AE features observed during strain hardening in various pure single- and poly-crystalline metals and alloys with different crystal lattices, alloying and loading conditions, etc.: [5-8] for FCC, [9, 10] for BCC and [11, 12 ] for HCP metals (many more can be listed). The ubiquitous finding across virtually all experimental studies is that AE during uniaxial monotonic plastic deformation of metals and alloys peaks shortly after the onset of microscopic yielding as is exemplified in Fig.1. This usually occurs at strains much smaller than those corresponding to the conventional yield stress $\sigma_{0.2}$ measured at 0.2% plastic strain. It is surprising that after many years of intensive research, the consensus has not been agreed upon the nature of this most prominent finding. Despite an ample similarity between the AE behaviour observed in different materials, there is still no commonly accepted phenomenological model or even a satisfactory qualitative description of the AE peak at the onset of yielding. The same applies to the following AE decay during strain hardening.

Gillis [13] noted that the elementary plastic power $dP_{pl}$ equals the inner product of the flow stress and plastic strain rate tensors, i.e. moving to scalars in the isotropic case $dP_{pl} = \tau d\dot{\gamma}$ , and introducing the Orowan's expression for the plastic strain rate

$$\dot{\gamma} = \rho_m b \langle v \rangle \tag{1}$$

where $\rho_m$ is the density of mobile dislocations, *b* is the magnitude of their Burgers vector, and $\langle v \rangle$ is their average velocity, he proposed that the plastic power generated by moving dislocations is proportional to the local stress and the dislocation flux. The greatest part of that power is dissipated as heat, while the rest can still be considered as a source for continuous acoustic emissions irradiated during plastic flow in metals. Despite the considerable differences in the approaches used in numerous early attempts to rationalise the AE behaviour in terms of the dislocation behaviour [14-18], many models converge in claiming that the AE energy emitted by moving dislocations is proportional to the density of mobile dislocations and their mean free path $\langle \Lambda \rangle$

$$\Delta E \sim \langle v \rangle^2 \rho_m \langle \Lambda \rangle \tag{2}$$

The additional factor, which arises in most formulations of AE-related parameters such as the amplitude, energy, power or *rms* voltage, is the mean velocity of dislocations $\langle v \rangle$. Fundamentally, the last relation is similar in a sense to that predicted by Scruby et al. [19] from the elasto-dynamic mechanics employed to calculate the elastic displacements arising at the epicentric sensor location in response to force dipoles representing the motion of a dislocation loop in the slip plane. Thus, the majority of the dislocation-based AE models appeal to the dislocation density as a proportionality coefficient for the AE energy (power, count rate, etc.) measured. James and Carpenter [20], however, challenged this relation in view of a substantial amount of experimental data which does not support such a simple proportionality. For

example, using *LiF* single crystals James and Carpenter demonstrated that the AE count rate was not proportional to the total (or mobile) dislocation density, but rather it was related the rate of change of the mobile dislocation density, although no model has been proposed to account for that.

Therefore, in spite of considerable efforts invested into understanding of the relation between the AE and plastic flow of materials, K. Ono [18] in his comprehensive review, has emphasized that the early models of dislocation-based AE sources, even if they were able to capture different specific features of the phenomenon qualitatively, were incomplete, and hard (or impossible) to compare with experiments. Carpenter and Heiple [21] at the same time emphasised that a serious drawback in the interpretation of a great deal of AE data was that AE is the microscopically sensitive phenomenon whereas the attempt to correlate it with the macroscopically measured loading diagrams, e.g. stress-strain curves, experienced substantial difficulties and inconsistencies.

The development of the microstructurally-based model of the AE phenomenon would substantially enhance the predictive capacity of the rapidly evolving AE technology, which is widely used in modern materials science laboratories and/or in industrial non-destructive integrity testing systems. Hence, in the present brief communication, we revisit the "classic" topic with the aim of developing a self-consistent experimentally-based phenomenological model describing the AE behaviour during plastic deformation of pure metals.

In a purely phenomenological approach paved by Gillis [13] and Ono [18] (see also the references therein), consider a single straight dislocation, which moves with the free path under the influence of a Peach-Köhler force [22] defined per length of the dislocation segment $L$: $\frac{F_{PK}}{L}=\tau b$. The free-flight dislocation velocity is given as $v=\dot{\Lambda}\equiv d\Lambda/dt$. The AE power caused by this elementary motion can be estimated as a fraction (small) of the total dissipated mechanical energy as:

$$\frac{p_{AE}}{L}\sim\frac{F_{PK}}{L}v=\tau b\dot{\Lambda} \tag{3}$$

Considering further that the mean free path of mobile dislocations in pure metals is determined by the density of immobile (forest) dislocations $\rho_f$, i.e. $\Lambda=1/\sqrt{\rho_f}$ [23], one obtains:

$$\dot{\Lambda}=-\frac{\dot{\rho}_f}{2\rho_f^{3/2}} \tag{4}$$

Combining it with the Taylor relation $\tau=\alpha Gb\sqrt{\rho_f}$ (here $G$ is the shear modulus and $\alpha$ is a numerical factor depending on the dislocation arrangement and the mode of deformation (typically of 0.1-0.4) [24-26], and the friction stress is neglected), which is ubiquitously fulfilled for virtually all conceivable

dislocation-dislocation interaction mechanisms and which tacitly assumes that the main strengthening effect is caused by the dislocations stored in the lattice, one obtains

$$\dot{\Lambda} = -\frac{\dot{\tau}}{\alpha G b \rho_f} \tag{5}$$

Plugging the last relation into Eq.(3), we obtain the relationship for the elementary dissipated AE power:

$$\frac{p_{AE}}{L} \sim \alpha G b^2 \frac{\dot{\tau}}{\tau} = \alpha G b^2 \frac{\dot{\sigma}}{\sigma} = \alpha G b^2 \frac{\theta}{\sigma} \dot{\varepsilon}_{pl} \tag{6}$$

with $\theta = \frac{d\sigma}{d\varepsilon}$ - the strain hardening rate. Pair of normal and shear stresses, $\sigma$ and $\tau$, and strains $\varepsilon$ and $\gamma$ are linked through the Taylor orientation factor $M$: $\sigma = M\tau$ and $\varepsilon = \gamma / M$, respectively. To account for all elementary motions of dislocations in the volume $V^*$, the last expression is multiplied by the total length of mobile dislocations $L_m = \rho_m V^*$, and the recorded AE power is determined as:

$$P_{AE} = \frac{p_{AE}}{L} L_m = \frac{p_{AE}}{L} \rho_m V^* \sim \dot{\varepsilon}_{pl} \theta \Lambda \rho_m V^* \tag{7}$$

Thus, when $\dot{\varepsilon}_{pl} = const$, the proportionality is anticipated between $P_{AE}$, $\theta$, $\Lambda$ and $\rho_m$, c.f. Eq.(2). The linear relation between $P_{AE}$ and $\dot{\varepsilon}_{pl}$ has long been recognised, c.f. [27, 28]. Equation (7) can be conveniently rewritten as

$$P_{AE} \sim \dot{\varepsilon}_{pl} \theta \Lambda \rho_m V^* = K_{AE} \rho_m \frac{\theta}{\sigma} \dot{\varepsilon}_{pl} = K_{AE} \rho_m \frac{\dot{\sigma}}{\sigma} \tag{8}$$

which predicts the proportionality between the experimentally measurable quantities – $P_{AE}$ and the $\theta / \sigma$ (or more generally $\dot{\sigma} / \sigma$) ratio derived from stress-strain data. Here the coefficient $K_{AE}$ incorporates all constants and accounts for a fraction of the total plastic power released in the AE form. The greatest advantage of this expression is that it is physically transparent and easily verifiable.

For the experimental validation, the I-shaped flat tensile specimens having the gauge length of 15×7×2 mm$^3$ were shaped by spark erosion from pure Ni, Al, Cu and Ag plates. The specimens were annealed in vacuum for 90min at different temperatures corresponding approximately to $0.85 \cdot T_m$, where $T_m$ is a melting temperature. As a result, coarse grain microstructures were produced with mean grain sizes ranging from 90 for Ag to 500μm for Ni, according to the electron back-scattered diffraction data [29], Table 1. These metals having the significantly different SFEs ranging from about 300mJ/m$^2$ for Ni to of 20mJ/m$^2$ for Ag are representative of a wide range of FCC metals with distinctly different dislocation mobility.

Uniaxial tensile testing was performed at the nominal strain rate of $2\times10^{-3}s^{-1}$ using a screw-driven testing machine with a clip-on extensometer. Considering that the elastic strain rate did not exceed $5\times10^{-5}s^{-1}$, the assumption that the plastic strain rate is constant and is approximately equal to $2\times10^{-3}s^{-1}$ is plausible. The AE signal was recorded by a wideband piezoelectric transducer NF AE-900S-WB mounted on the specimen surface. The AE signal amplified by 60dB in the frequency band from 100 to 900kHz was continuously recorded by a PCI-2 board (MISTRAS, USA) at the sampling frequency of 2MHz. The power spectral density (PSD) function $G(f)$ was calculated using a periodogram technique with a 40kHz rectangular spectral smoothing window. The following two quantities were introduced to characterise the AE PSD: the *power* referred to 1Ohm nominal impedance, $P_{AE}=\int_{f_{\min}}^{f_{\max}}G(f)\,df$, and the *median frequency* $f_m$ defined by the implicit equation $\int_0^{f_m}G(f)\,df=\int_{f_m}^{\infty}G(f)\,df$. Both $P_{AE}$ and $f_m$ were obtained from $G(f)$ after subtraction of the PSD of the laboratory noise (see [30] for details).

Results of mechanical testing paired with AE measurements are presented in Fig.1. For all metals tested, the AE power exhibits the familiar behaviour with a pronounced sharp maximum at the onset of plastic yielding and a gradual decay afterwards. The AE power peaks when the most rapid hardening occurs. In this sense, it correlates with $\theta$ as can be seen in Fig.1. The correlation between $P_{AE}$ and $\theta$ has been noticed in several reports [30-32] for Cu single crystals though it was confirmed only at the AE maximum. However, no apparent functional relationship has been found between $P_{AE}$ and $\theta$ from data shown in Fig.1. On the other hand, Fig.2a shows that, beyond the onset of yielding, the linear relationship does exist between $P_{AE}$ and the reduced strain hardening rate $\theta/\sigma$ in excellent agreement with Eq.(8). This agreement tacitly assumes that the mobile dislocation density saturates after initial rapid accumulation, and $\rho_m(\varepsilon)=const$ through the rest of the test. The strong assumption of the strain independent density of mobile dislocations is generally accepted to be valid [33, 34] outside the micro-yielding stage (note that this was an essential assumption in the dislocation kinetic model developed by Bergström [23]). This can be argued from the common thermal activation analysis of the dislocation glide assuming the Arrhenius-type equation for the dislocation velocity and, therefore, for the plastic strain rate

$$\dot{\gamma}_{pl}=\dot{\gamma}_0\exp\left(-\frac{\Delta G_0-\tau^* V_a}{k_B T}\right) \tag{9}$$

where $k_B$ is the Boltzmann's constant, $T$ is the absolute temperature, and the activation process is controlled by the free activation enthalpy $\Delta H(\tau^*)=\Delta G_0-\tau^* V_a$, which is explicitly dependent on the thermal component of the flow stress $\tau^*$ acting on the glide dislocations during overcoming of short-range obstacles; $\Delta G_0$ represents the stress independent activation energy, and $V_a$ is known as the

activation volume. The scaling factor $\dot{\gamma}_0$ [34, 35] is proportional to $\rho_m$ and the attempt frequency against the obstacle, which is a material's constant of the order of the Debye frequency. Since $\dot{\gamma}_0$ has not been found to be a function of strain or stress, it is commonly assumed to be independent of stress and temperature, and, therefore, so does the mobile dislocation density. This is further corroborated by a large body of experimental observations of the evolution of the AE power spectral density. Vinogradov et al. [1] have demonstrated that the AE PSD shifts to the high-frequency domain so that the spectral median frequency $f_m$ scales linearly with the flow stress $\sigma$ during uniform elongation. Considering the spectrum of the weakly correlated stationary random AE process [1], its median frequency was inversely related to the relaxation time in the dislocation ensemble, which was expressed by the $\langle\Lambda\rangle/\langle v\rangle$ ratio, and using the Orowan's and Taylor's relations, one obtained the simple phenomenological relation for $f_m$

$$f_m \sim \frac{\langle v\rangle}{\langle\Lambda\rangle} = \frac{\dot{\gamma}_{pl}}{b\rho_m}\sqrt{\rho} \sim \frac{\tau}{\rho_m}\dot{\gamma}_{pl} = \frac{\sigma}{\rho_m}\dot{\varepsilon}_{pl} \tag{10}$$

The experimentally observed proportionality between $f_m$ and $\sigma$ predicted by the last expression is illustrated by the $f_m$ *vs* $\sigma$ plot in Fig.2b for all materials tested and in more details in Fig.3 for copper. We should notice that this proportionality holds only if $\rho_m$ is constant. At the early stage when mobile dislocations are generated, this proportionality breaks down, and the initial pronounced drop in $f_m$ is obviously attributed to the rapid growth of $\rho_m$, generally leading to the AE peak which is observed nearly concomitantly with the $f_m$ minimum, Fig.3.

Finally, it is instructive to notice that Eq.(8) explicitly implies that $P_{AE}$ is a linear function of $\rho_m$ though the $P_{AE}(\rho_m)$ functional dependence is admittedly more complex than it was predicted in earlier models, c.f. Eq.(2), since the other entering variables depend on $\rho_m$ too. Assuming that $\rho_m$ is a constant fraction of the total dislocation density $\rho$, which scales with the mechanical stress according to the Taylor relation as $\rho_m \sim \sigma^2$, the elementary rearrangement of the last expression yields that $P_{AE} \sim \rho_m \frac{\dot{\sigma}}{\sigma} \approx \sigma\dot{\sigma} \sim \frac{d\rho}{dt}$ as it was heuristically suggested by James and Carpenter [20]. The assumption that $\rho_m \approx \rho$ is, of course, crude, which can be argued more or less reasonably for the early stage of deformation of a well-annealed poly- or single-crystals only. However, in the forthcoming publication, we endeavour to demonstrate it rigorously that the proportionality $P_{AE} \sim \frac{d\rho}{dt}$ holds for the AE peak indeed, but not elsewhere.

Equation (8) allows for the additional independent verification of the model by using the stress-rate controlled experiments at $\dot{\sigma} = const$. This was done for Cu samples tested in tension on a servo-

hydraulic Instron 8082 machine at $\dot{\sigma} = 5 MPa / s$. Figure 4 shows that the AE power peaks at 6s due to the rapid increase of $\rho_m$ entering Eq.(8) (a) and, after that, the linear relation is confirmed between $\dot{\sigma} / \sigma$ and $P_{AE}$ (b) in excellent agreement with Eq.(8).

In conclusion, considering AE as a phenomenon reflecting the elastic energy dissipation process occurring in deforming metals during dislocation-mediated plastic deformation, we demonstrate that the AE power scales with the dislocation density in a complex way determined by dislocation interactions during strain hardening. The relationship between the AE power and the strain hardening behaviour in the form $P_{AE} \sim \rho_m \frac{\theta}{\sigma} \dot{\varepsilon}_{pl}$ was derived and experimentally verified for several FCC metals with different SFE. Despite its simplicity, this proposed phenomenological relation captures most of the salient features of the AE behaviour of pure metals, dilute solid solutions and alloys before strain localisation and/or plastic instability sets in. This will be further unfolded in the upcoming full-length publication where the effects of loading conditions and metallurgical factors will be incorporated explicitly in the proposed model framework within a time-proven dislocation kinetics approach. The important challenges, which have yet to be addressed in modelling include the effects of texture, impurities and plastic instabilities, which strongly affect the AE behaviour in structural materials [36-38]. With the appropriate calibration, this offers a robust and consistent interpretation of the AE data, equipping materials scientists with the new functionality of the modern AE technology, and enabling in-situ monitoring and the analysis of dislocation kinetics in materials.

**Acknowledgements.** Financial support from the Ministry of Science and Higher Education of Russia according to the contract N 11.5281.2017/8.9 is gratefully appreciated. The authors are thankful to M. Linderov and A. Danyuk for their skilful and enthusiastic help with experiments.

## References

[1] A. Vinogradov, I.S. Yasnikov, Y. Estrin, Journal of Applied Physics, 115 (2014) 233506
[2] A. Müller, C. Segel, M. Linderov, A. Vinogradov, A. Weidner, H. Biermann, Metallurgical and Materials Transactions A, (2015) 1-16.
[3] D. Drozdenko, J. Bohlen, S. Yi, P. Minárik, F. Chmelík, P. Dobroň, Acta Materialia, 110 (2016) 103-113.
[4] T. Richeton, J. Weiss, F. Louchet, Nature Materials, 4 (2005) 465-469.
[5] C. Scruby, H. Wadley, J.E. Sinclair, Philosophical MagazineA, 44 (1981) 249-274.
[6] J. Baram, M. Rosen, Materials Science and Engineering, 47 (1981) 243-246.
[7] Z.I. Bibik, A.L. Samsonic, V.M. Andronov, Fiz Met Metalloved, 64 (1987) 412-415.
[8] M.A. Krishtal, D.L. Merson, A.V. Katsman, M.A. Vyboyschchik, Phys Met Metallography, 66 (1988) 169-175.

[9] F.P. Higgens, S.H. Carpenter, Acta Metallurgica, 26 (1978) 133-139.
[10] A. Lazarev, A. Vinogradov, J. of Acoustic Emission, 27 (2009) 144-156.
[11] P. Dobroň, J. Bohlen, F. Chmelík, P. Lukáč, D. Letzig, K.U. Kainer, Materials Science and Engineering: A, 462 (2007) 307-310.
[12] M. Friesel, S. Carpenter, Metall and Mat Trans A, 15 (1984) 1849-1853.
[13] P.P. Gillis, Dislocation Motions and Acoustic Emissions, in: Acoustic Emission, ASTM STP 505, American Society for Testing and Materials, 1972, pp. 20-29.
[14] A.S. Tetelman, in: US-Japan Joint Symposium on Acoustic Emission, English volume, Japan Industrial Planning Association, 1972, pp. 1-46.
[15] K. Malen, L. Bolin, physica status solidi b, 61 (1974) 637-645.
[16] N. Kiesewetter, P. Schiller, physica status solidi a, 38 (1976) 569-576.
[17] N. Kiesewetter, Scripta Metallurgica, 8 (1974) 249-252.
[18] K. Ono, in: K. Ono (Ed.) Fundamentals of Acoustic Emission, Univeristy of California, CA, UCA, 1979.
[19] C.B. Scruby, H.N.G. Wadley, J.J. Hill, Journal of Physics D, 16 (1983) 1069-1083.
[20] D.R. James, S.H.Carpenter, Journal of Applied Physics, 42 (1971) 4685-&.
[21] S.R. Carpenter, C.R. Heiple, in: K. Ono (Ed.) Fundamentals of Acoustic Emission, Univeristy of California, CA, USA, 1979, pp. 49-104.
[22] J.P. Hirth, J. Lothe, Theory of dislocations, 2nd ed., Wiley, New York, 1982.
[23] Y. Bergström, Materials Science and Engineering, 5 (1970) 193-200.
[24] U.F. Kocks, H. Mecking, Progress in Materials Science, 48 (2003) 171-273.
[25] M. Sauzay, L.P. Kubin, Progress in Materials Science, 56 (2011) 725-784.
[26] H. Mughrabi, Current Opinion in Solid State and Materials Science, 20 (2016) 411-420.
[27] R.M. Fisher, J.S. Lally, Canadian Journal of Physics, 45 (1967) 1147-1159.
[28] H. Hatano, Journal of Applied Physics, 47 (1976) 3873-3876.
[29] A.V. Danyuk, D.L. Merson, I.S. Yasnikov, E.A. Agletdinov, M.A. Afanasiev, A. Vinogradov, Lett. Mater., 7 (2017) 437-441.
[30] A. Vinogradov, M. Nadtochiy, S. Hashimoto, S. Miura, Materials Transactions JIM, 36 (1995) 496-503.
[31] A. Vinogradov, M. Nadtochiy, S. Hashimoto, S. Miura, Materials Transactions JIM, 36 (1995) 426-431.
[32] A. Vinogradov, I.S. Yasnikov, Acta Materialia, 70 (2014) 8-18.
[33] T.H. Alden, Metall Trans A, 18 A (1987) 51-62.
[34] P. van Liempt, Journal of Materials Processing Technology, 45 (1994) 459-464.
[35] L. Hollang, E. Hieckmann, D. Brunner, C. Holste, W. Skrotzki, Materials Science and Engineering A, 424 (2006) 138-153.
[36] K. Máthis, G. Csiszár, J. Čapek, J. Gubicza, B. Clausen, P. Lukáš, A. Vinogradov, S.R. Agnew, International Journal of Plasticity, 72 (2015) 127-150.
[37] I.V. Shashkov, M.A. Lebyodkin, T.A. Lebedkina, Acta Materialia, 60 (2012) 6842-6850.
[38] M. Lebyodkin, K. Amouzou, T. Lebedkina, T. Richeton, A. Roth, Materials, 11 (2018) 1061.
[39] L.E. Murr, Interfacial Phenomena in Metals and Alloys, Addison-Wesley, London, UK, 1975.
[40] J.A. Venables, Journal of Physics and Chemistry of Solids, 25 (1964) 685-692.
[41] M. Ahlers, Metallurgical Transactions, 1 (1970) 2415-2428.

Table 1. Properties of metals tested and experimental results.

| Properties | Metal | | | |
|---|---|---|---|---|
| | Ni | Al | Cu | Ag |
| Annealing temperature, K | 1470 | 640 | 1070 | 1170 |
| Stacking Fault Energy, *SFE* $\gamma_{SFE}$, mJ/m$^2$ [39-41] | 300 | 170-250 | 40-70 | 18-25 |
| Mean grain size, $d$ /μm | 500 ± 300 | 200 ± 100 | 100 ± 35 | 90 ± 70 |
| Yield stress, $\sigma_{0.2}$ / MPa | 42.5 | 19.9 | 20.0 | 15.3 |
| Ultimate tensile strength, $\sigma_{UTS}$ / MPa | 340 | 43.2 | 213 | 137 |
| Elongation at break, $\varepsilon_f$ | 0.40 | 0.50 | 0.47 | 0.49 |
| Peak of the AE power, $P_{AEmax}$, μV$^2$/Ohm | 30 | 43 | 82 | 126 |

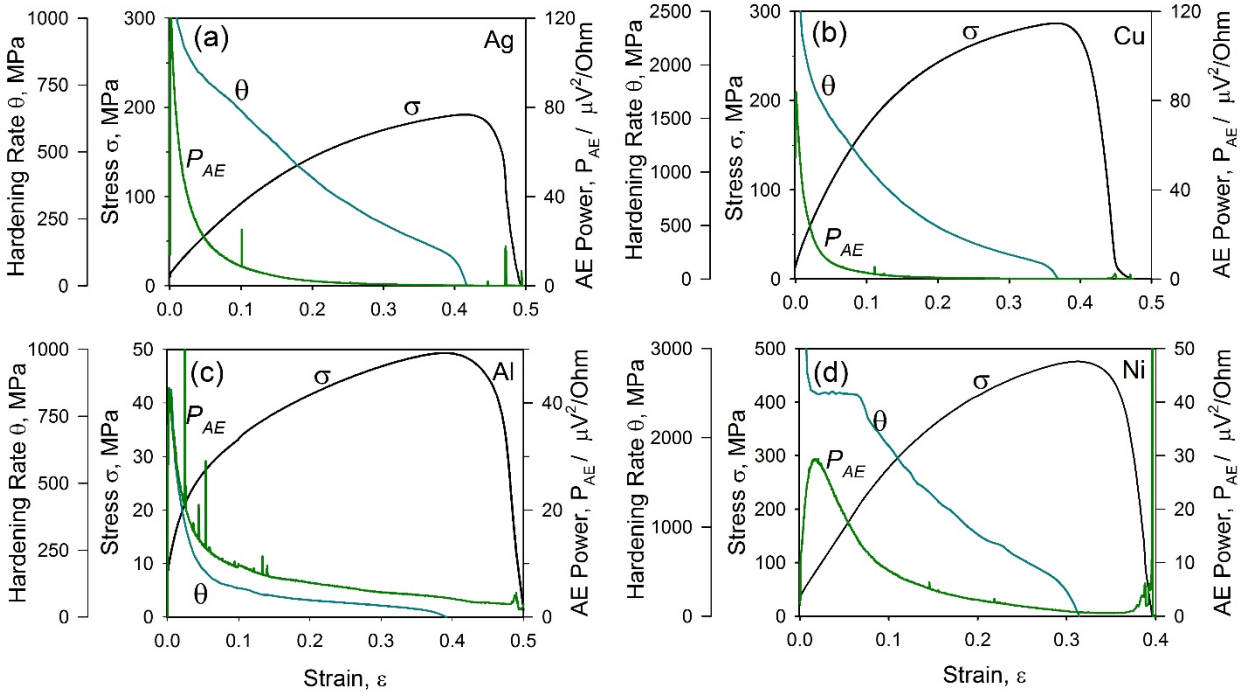


**Figure 1.** Hardening curve (black), strain hardening coefficient (cian), and AE power (green) for different samples: (a) Ag; (b) Cu; (c) Al; (d) Ni

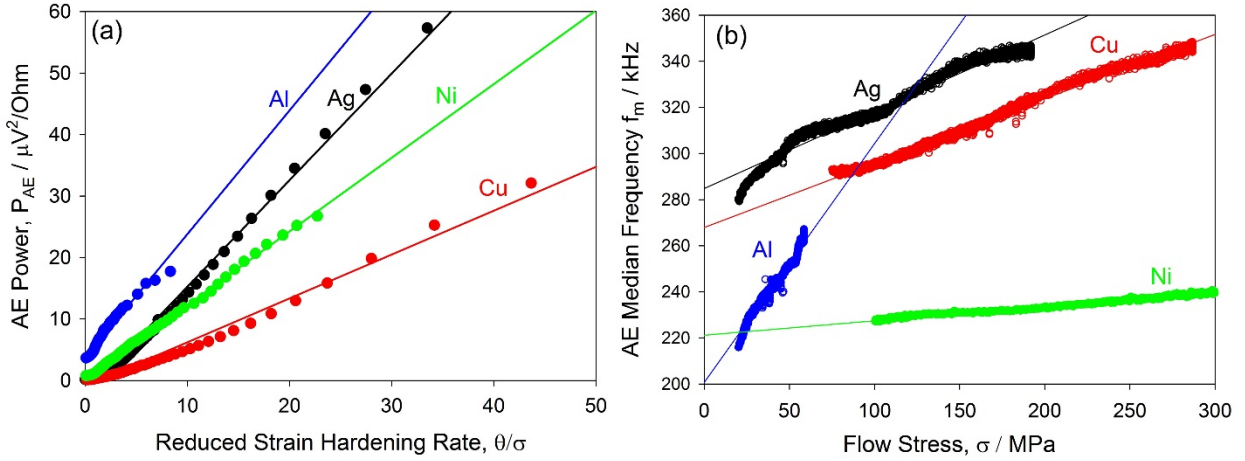


**Figure 2.** Dependence of the AE power $P_{AE}$ on the reduced strain hardening rate $\theta/\sigma$ (a) and the AE median frequency $f_m$ on the flow stress $\sigma$ (b) for all pure metals with different stacking fault energies. Straight lines are obtained by the least square linear curve fitting method.

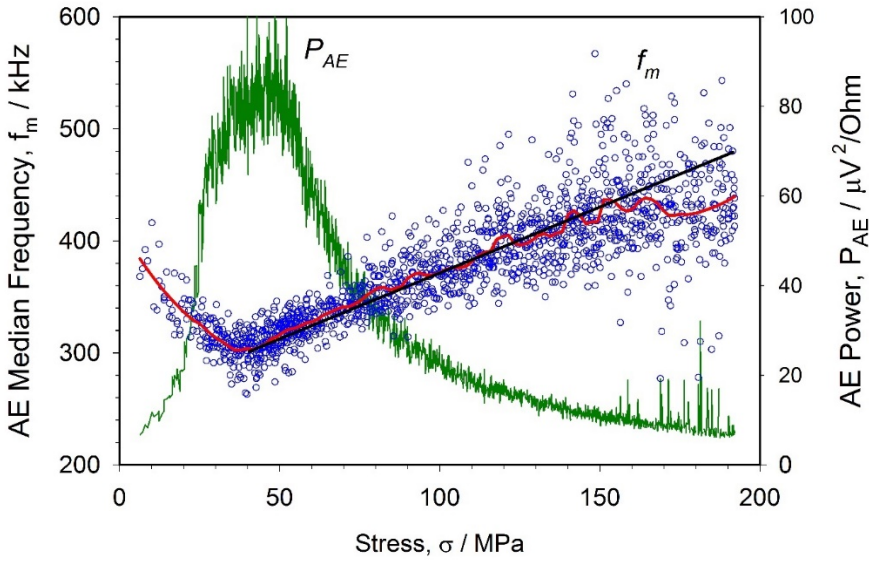


**Figure 3.** Typical example showing the AE power $P_{AE}$ and median frequency $f_m$ as a function of the flow stress in a pure copper polycrystal. Each open blue circle shows the result of $f_m$ calculation for a 4096 points realisation of the continuously recorded AE signal. The red solid line represents the result of Loess smoothing, while the straight black line is the result of linear curve fitting with the regression coefficient $r^2$=0.998.

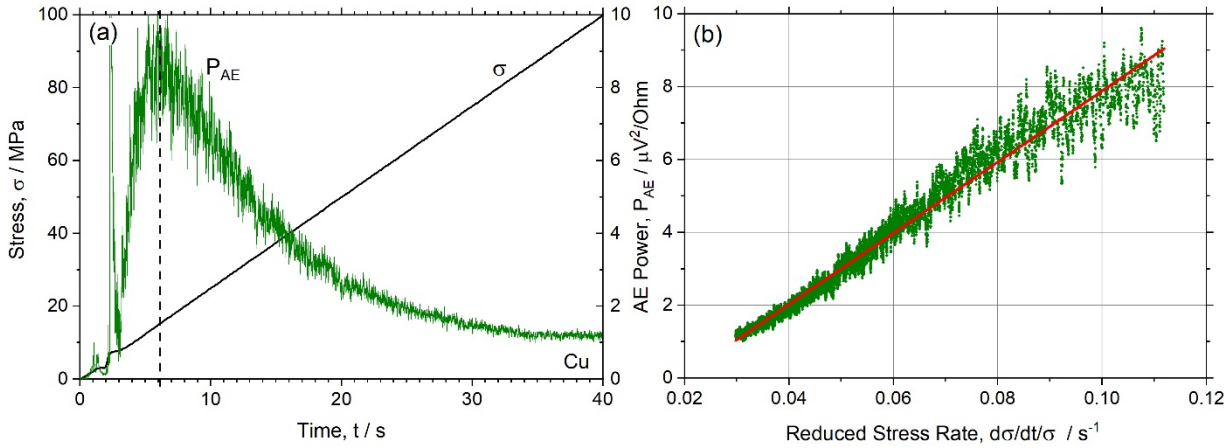


**Figure 4.** The behaviour of the AE power $P_{AE}(t)$ as a function of deformation time in a pure copper plocrystal tested under constat stress-rate conditions $\dot{\sigma} = const$ (a). (b) shows the linear relation between $P_{AE}$ and $\dot{\sigma}/\sigma$ for the decaying part of the $P_{AE}(t)$ curve (experimental points are taken to the right from the dashed line on (a)), as predicted by Eq.(8)